Author accepted manuscript
Final version: *Biochem J*. 2017 Feb 15;474(4):571-587

DDX3 directly regulates TRAF3 ubiquitination and acts as a scaffold to coordinate assembly of signalling complexes downstream of MAVS.

Lili Gu, Anthony Fullam, Niamh McCormack, Yvette Höhn, and Martina Schröder

Institute of Immunology, Maynooth University, Maynooth, Co. Kildare, Ireland

Corresponding author:

Martina Schroeder, Institute of Immunology, National University of Ireland Maynooth, Maynooth, Co. Kildare, Ireland, Tel:+353-1-708-6853, Fax: +353-1-708-6337, email: martina.schroeder@nuim.ie

Abstract

The human DEAD-box helicase 3 (DDX3) has been shown to contribute to type I interferon induction downstream of anti-viral pattern recognition receptors (PRRs). It binds to TANK-binding kinase 1 (TBK1) and IκB-kinase-ε (IKKε), the two key kinases mediating activation of Interferon regulatory factor (IRF) 3 and IRF7. We previously demonstrated that DDX3 facilitates IKKε activation downstream of RIG-I and then links the activated kinase to IRF3. In this study, we probed the interactions between DDX3 and other key signalling molecules in the RIG-I pathway and identified a novel direct interaction between DDX3 and TRAF3 mediated by a TRAF-interaction motif in the N-terminus of DDX3, which was required for TRAF3 ubiquitination. Interestingly, we observed two waves of K63-linked TRAF3 ubiquitination following RIG-I activation by Sendai Virus infection (SeV), both of which were suppressed by DDX3 knockdown. We also investigated the spatiotemporal formation of endogenous downstream signalling complexes containing the MAVS adaptor, DDX3, IKKε, TRAF3 and IRF3. DDX3 was recruited to MAVS early after SeV infection, suggesting it might mediate subsequent recruitment of other molecules. Indeed, knockdown of DDX3 prevented formation of TRAF3-MAVS and TRAF3-IKKε complexes. Based on our data, we propose that early TRAF3 ubiquitination is required for formation of a stable MAVS-TRAF3 complex, while the second wave of TRAF3 ubiquitination mediates IRF3 recruitment and activation. Our study characterises DDX3 as a multifunctional adaptor molecule that coordinates assembly of different TRAF3, IKKε and IRF3-containing signalling complexes downstream of MAVS. Additionally, it provides novel insights into the role of TRAF3 in RIG-I signalling.

Short summary
We identified a novel direct interaction between DDX3 and TRAF3 important for signalling by the anti-viral pattern recognition receptor RIG-I, and characterised spatiotemporal formation of endogenous downstream signalling complexes, providing novel insights into the role of TRAF3 in RIG-I signalling.

Short title:

Human DDX3 interacts directly with TRAF3

Keywords: Interferon, RIG-like helicases, TRAF, Ubiquitination, DEAD-box protein

Abbreviations: Aa, amino acid; CK, Casein Kinase; GST, Glutathione-S-Transferase; HA, hemagglutinin; HEK, Human embryonic kidney; IFN, interferon; IKK, IkB kinase; IP, immunoprecipitation; IRF, interferon regulatory factor; MAVS, mitochondrial antiviral signalling; mt, mutant; Ni-Ag, Nickel-Agarose; NSC, non-silencing control; PRR, pattern recognition receptor; RIG, retinoic-acid inducible gene; RLH, RIG-like Helicase; SeV, Sendai Virus; shRNA, short hairpin RNA; siRNA, small interfering RNA; TBK, TANK-binding kinase; TLR, Toll-like receptor; TRAF, TNF receptor associated factor; WB, western blot; wt, wild-type

Introduction

During viral infections, viral nucleic acids are detected by a range of intracellular pattern recognition receptors (PRRs). A hallmark of these anti-viral PRRs is the activation of signalling pathways that lead to production of type I interferons. Induction of type I IFN gene promoters requires interferon regulatory factor (IRF)3 or IRF7, transcription factors that dimerise and translocate into the nucleus following phosphorylation of crucial serine residues. The IKK-related kinases IKKϵ and TBK1 phosphorylate IRF3 and IRF7 downstream of anti-viral PRRs, including Toll-like receptor (TLR)3, the RIG-like helicases (RLHs), and cytoplasmic DNA receptors [1-4]. Interestingly, it was demonstrated that all TLRs activate TBK1 and IKKϵ via a pathway dependent on MyD88 and the canonical IKKs, yet IRF3 phosphorylation and induction of type I IFNs only occur downstream of TLR3 and TLR4 [5]. This suggested that activation of the IKK-related kinases is required but not sufficient for IRF3 activation, and it has been proposed that an additional adaptor molecule links the activated IKK-related kinases to IRF3 in cells [5]. We have previously demonstrated that the DEAD-box protein DDX3 facilitates IKKϵ activation, and also links activated IKKϵ to IRF3 to enable IRF3 phosphorylation [6]. As a DEAD-box helicase, DDX3 can act as an RNA remodelling enzyme and has functions in RNA metabolism [7]. However, its role in IRF3 activation and type I IFN induction did not require its enzymatic activity [8, 9], in line with a function as signalling adaptor. There are two functional DDX3 genes in the human genome, one on the X-chromosome (DDX3X) and one on the Y-chromosome (DDX3Y). This work, and also our previous work [6, 8], has been carried out with DDX3X, which we refer to as DDX3 for the remainder of the text. DDX3Y protein was proposed to only be expressed in the male germline [10]. Another key signalling molecule for IFN induction is TRAF3, which is part of the TLR and RLH pathways and required for IRF3 activation [11, 12]. TRAF3 has also been suggested as a prime candidate for providing the missing link between IKKε/TBK1 and IRF3 activation [5]. On the other hand, a lot of studies support an upstream role for TRAF3 in the activation of IKKε/TBK1, e.g. it has been shown to bind to the adaptors TRIF and MyD88 which mediate TLR signalling to IRF3/7 activation [12], as well as to MAVS which carries out an equivalent adaptor function in the RLH signalling pathway [13], and to facilitate recruitment of IKKε/TBK1 to these adaptors. TRAF3, like all TRAF proteins, can contribute to signalling pathways either by acting as an adaptor molecule or through its E3 ligase activity, which catalyses the addition of K63-linked ubiquitin chains to specific substrates [14]. K63-linked ubiquitin chains provide docking sites for the recruitment of additional signalling molecules, and therefore constitute important posttranslational modifications that regulate signal transduction events. This is in contrast to K48-linked ubiquitination which marks proteins for proteasomal degradation. Activation of TRAF3 involves its oligomerisation followed by K63-linked auto-ubiquitination, which has been shown to be required for IFN induction [15]. It is not fully understood how exactly ubiquitination of TRAF3 contributes to IFN induction, but it was suggested to mediate interaction with IKKε/TBK1 [16]. In summary, while the overall importance for TRAF3 in IFN induction pathways downstream of several different PRR pathways is well established, its exact placement in the pathway and the role of its E3 ligase activity are not clear.

In this study, we describe the identification of a novel direct interaction between DDX3 and TRAF3 through an N-terminal TRAF-binding motif in DDX3. We show that the DDX3-TRAF3 interaction is required for

K63-linked TRAF3 ubiquitination and *ifnb* promoter activation following activation of the RIG-I pathway. We also studied the spatiotemporal formation of endogenous signalling complexes following activation of the RIG-I pathway by Sendai virus infection. Our data suggest a non-linear relationship for DDX3 and TRAF3 in the pathway, and supports the existence of two distinct TRAF3 ubiquitination events which may be required for the formation of different signalling complexes. Thus, our data could help to explain the ambiguity surrounding the positioning of TRAF3 in IRF3 activation pathways. Most importantly though, it identifies an additional novel function for DDX3 in the coordination of multiple signalling complexes following RIG-I activation by viral infection.

Experimental

Plasmids, recombinant proteins and antibodies

The expression constructs pCMV-HA-DDX3, pCMV-Myc-DDX3, pHis2-DDX3 (full-length and truncations) and pGST2-DDX3 have been described in our previous studies [6, 8]. The P142/E144A mutation was introduced into pCMV-HA-DDX3 and pHis-DDX3 (1-408) following instructions for the QuikChange Site-Directed Mutagenesis Kit (Agilent), except for using Pfusion™ HiFi polymerase (New England Biolabs). Introduction of the point mutations appeared to change mobility of the DDX3 protein in SDS-PAGE. However, the constructs have been fully sequenced to rule out additional mutations and sequencing confirmed its identity. IKKε–flag, MAVS-flag and TRAF3-flag plasmids were kindly provided by Dr Kate Fitzgerald (University of Massachusetts Medical School, Worcester, MA). Plasmids for TRAF3-flag truncations were kindly provided by Prof Carl Ware (Sandford Burnham Medical Research Institute) [17], the plasmid for the TRAF3 C68A/H70A mutant was a kind gift from Prof Michael Karin (University of California, San Diego). Constructs for flag-Sintbad, flag-TANK and flag-NAP1 were provided by Dr Felix Randow (MRC Laboratory of Molecular Biology, Cambridge, UK) [18]. The expression construct for HA-tagged K63o(nly) Ubiquitin was provided by Dr Marion Butler (NUI Maynooth, Ireland). Recombinant TRAF3 was purchased from Novus Biologicals. The IKKϵ/TBK1 inhibitor BX795 was purchased from Invivogen Europe (Cayla, France).

The antibodies used were anti-flag M2 mAb (Sigma-Aldrich), anti-Myc mAb clone 9E10 (Sigma-Aldrich), anti-HA mAb (Covance), anti-DDX3 (Santa Cruz or Bethyl Laboratories), anti-Cardif (MAVS) (pAb AT107, Enzo Life Sciences), anti-TRAF3 (Santa Cruz), anti-IKKε (Abcam, Cambridge, UK), anti-IRF3 (IBL), anti-His (Sigma-Aldrich), anti K63-Ubiquitin (Cell Signaling Technologies), and anti-GST (Promega). Sendai Virus Cantell strain was obtained from Charles River Laboratories and used at a concentration of 80 HA U/ml.

Cell culture and Transfection

HEK293T and A549 cells were maintained in Dulbecco's Modified Eagle Medium (DMEM) with Glutamax™ (Gibco), supplemented with 10% foetal calf serum and 50 ng/ml gentamycin (Sigma-Aldrich). Transient DNA transfections for immunoprecipitations and pull-downs were performed using the Calcium Phosphate method. Total amount of DNA was kept constant by addition of empty vector.

shRNA knockdown of DDX3

Lentiviral particles were generated by transfecting HEK293T cells with either pTRIPZ shDDX3 (V2THS_228965, Thermo Scientific) or the corresponding non silencing control (NSC), and the packaging vectors psPAX2 and pMD2.G in the presence of chloroquine sulfate (5 μM). 16 h after transfection, the supernatant was removed and 5 ml fresh medium was added. Lentivirus-containing supernatants were harvested 24 h and 48 h and concentrated using PEG-precipitation. For generating knockdown cells, A549 or HEK293T cells were plated at $3x10^5$ cells/ml into a 6wp. 24h later the medium was replaced with 1 ml medium containing 4 μg/ml protamine sulphate. shDDX3 or NSC lentivirus was added at an MOI of 10. To create stable cell lines, the medium was replaced 24 h after transduction with 2 ml culture medium containing 1.5 μg/ml puromycin. After selection, the cells were also routinely kept in culture in the presence

of puromycin. For use in experiments, cells were cultured in the absence of puromycin and DDX3 knockdown was induced by the addition of 0.5 μg/ml doxycycline for 48 h.

siRNA knockdown of TRAF3

For siRNA knockdown of endogenous human TRAF3, the Dharmacon siGENOME SMARTpool TRAF3 or a non-targeting control SMARTpool were used (Thermo Fisher). Approximately $4x10^5$ HEK293T cells were transfected with the SMARTpool siRNA (25nM) in 6wp using Lipofectamine™ 2000 (Invitrogen), according to manufacturer's instructions. 48 h after transfection, cell lysates were prepared, used for co-immunoprecipitations, and analysed by SDS–PAGE and immunoblotting.

GST or His pull-down assays

Bacterial expression constructs for His- or GST-tagged proteins were transformed into *E. coli* BL21 (DE3). Protein expression was induced by IPTG, and recombinant proteins were purified using either Nickel-Agarose (Qiagen) or Glutathione-Sepharose (Chromatrin Ltd, Dublin, Ireland). For pull-downs, equal amounts of the different His- or GST- tagged fusion proteins were used, as estimated by SDS–PAGE and Coomassie staining prior to use. Cell lysates containing flag-tagged protein expressed in HEK293T cells were incubated with the purified His- or GST-tagged proteins coupled to Nickel-Agarose or Glutathione-Sepharose respectively. Alternatively, 2 μg of recombinant TRAF3 was used in the pulldown with His-DDX3. Protein complexes were precipitated and washed thoroughly, before being subjected to SDS–PAGE and Western-Blot analysis. Control pulldowns were carried out with GST protein coupled to Glutathione-Sepharose or empty Ni-Agarose beads for GST- and His-pulldowns respectively.

Co-immunoprecipitation assays

Co-immunoprecipitations were performed from cell lysates of transiently transfected HEK293T cells, which were harvested 24 h after transfection. Alternatively, for endogenous co-IPs, lysates from A549 cells seeded in 10 cm dishes were prepared following SeV infection. Cells were lysed in IP lysis buffer (50mM Hepes pH 7.4, 150 mM NaCl, 2 mM EDTA, 1% NP-40, 10% Glycerol, 10 mM NaF, 10 mM DTT, protease inhibitors). Cell lysates were incubated with 20 μl of Flag-M2 Agarose (Sigma-Aldrich) or Protein G agarose (Sigma-Aldrich) that had been pre-coupled with 2 μl of the relevant antibodies at 4 °C overnight and blocked with 5% BSA. The immunoprecipitated protein complexes were washed thoroughly and then eluted by boiling in Laemmli sample buffer, before being subjected to SDS–PAGE and Western-Blot analysis.

Detection of endogenous TRAF3 ubiquitination

HEK293T cells (shDDX3 or NSC shRNA) were lysed in RIPA buffer following infection with SeV. Cell lysates were boiled for 5min in the presence of 1% SDS. TRAF3 was immunoprecipitated from the denatured cell lysates, and precipitates were subjected to SDS-PAGE and Western Blot analysis with an antibody specific for K63-linked ubiquitin chains (Cell Signaling Technologies).

Reporter gene assays

Ifnb promoter induction was measured in HEK293 cells seeded into 96-well plates (2×10^4 cells per well) and transfected 24 h later with expression vectors and luciferase reporter gene constructs, using GeneJuice (Merck/Millipore). 60 ng of an *ifnb* promoter Firefly luciferase reporter gene construct was used in conjunction with 20 ng of a pGL3-Renilla luciferase construct (both provided by Andrew Bowie, Trinity College Dublin). The total amount of DNA transfected was kept constant at 230ng/well by addition of matching empty vector DNA. Firefly and Renilla Luciferase activity was measured 24 h after transfection. Alternatively, cells were infected with SeV 24 h after stimulation and harvested after a further 16 h. Renilla Luciferase readings were used to normalise for transfection efficiency. Data are expressed as mean fold induction ± SD relative to control levels, for an individual experiment performed in triplicate.

Data representation

All data shown are representative of at least two independent repeat experiments, most are representative of 3-5 repeat experiments. Luciferase reporter gene assays are representative of at least 3 independent repeat experiments. Where a black box has been placed around Western Blot Results, this indicates that they were taken from the same original autorad exposure, and can thus be directly compared for intensity. Any adjustments for brightness and contrast have been applied evenly across the whole (boxed) panel.

Results

DDX3 directly interacts with TRAF3

Our previous papers demonstrated that DDX3 is a positive regulator of type I IFN production in antiviral PRR signalling pathways [6, 8], which has also been confirmed by others [9, 19-21]. We showed that DDX3 directly interacts with IKKϵ and IRF3, and thereby facilitates IRF3 phosphorylation by IKKϵ [6]. During this research that aimed to place DDX3 firmly into the signalling pathway leading to type I IFN induction downstream of RIG-I, we also tested whether DDX3 interacts with other important signalling molecules in this pathway. We expressed flag-tagged IKKϵ (as a positive control), MAVS, Sintbad, NAP1, TANK and TRAF3 in HEK293 cells and carried out pull-down assays with either recombinant GST-tagged or His-tagged DDX3. GST-DDX3 pulled down IKKϵ as expected; and it also interacted with TRAF3 and (weakly) with Sintbad, but not with TANK or NAP1 (Figure 1A). Despite the fact that a larger amount of GST protein compared to GST-DDX3 protein was present in control pulldowns (GST and GST-DDX3 signals shown in Figure 1A were detected on the same autoradiograph), we did not observe binding of TRAF3, IKKε or Sintbad to the GST control, indicating that the observed interactions were specific for DDX3. In pulldown experiments with His-tagged DDX3, we also confirmed an interaction with MAVS (Figure 1A), which has previously been described by Oshiumi *et al*. [20]. In pulldowns with His-tagged DDX3, control pulldowns were carried out with empty Ni-Agarose beads (NiAg). There was no non-specific binding of MAVS to the Ni-Agarose matrix, again suggesting a specific interaction with DDX3. We were particularly interested in the observed interaction with TRAF3, because TRAF3 is a crucial signalling molecule for the activation of IRF3. We therefore confirmed and mapped the DDX3-TRAF3 interaction using pulldown assays with recombinant His-tagged DDX3 truncations (Figure 1B). Full-length His-tagged DDX3 (aa 1-662) pulled down ectopically expressed flag-tagged TRAF3 from HEK293 cell lysates as expected, and the N-terminal domain of DDX3 (aa 1-408) also pulled down flag-TRAF3, while the C-terminal domain of DDX3 (aa 409-662) did not. Further truncations of the N-terminal domain revealed that TRAF3 still interacted with DDX3 139-408, but not with DDX3 172-408 (Figure 1B). The interaction of TRAF3 with the 139-408 DDX3 truncation made it unlikely that the this interaction is bridged by IKKϵ, as IKKϵ fails to interact with the 139-408 truncation mutant (it binds to a region between amino acids 100 and 110 of DDX3) [6]. To address the question whether DDX3 and TRAF3 directly interact, we next carried pulldown assays using purified recombinant His-tagged DDX3 and GST-tagged TRAF3 purchased from Novus Biologicals. As shown in Figure 1C, recombinant GST-TRAF3 was pulled down with His-tagged DDX3, but did not bind to Ni-Agarose beads in the absence of His-DDX3, indicating that DDX3 and TRAF3 can directly interact. We next determined which domain of TRAF3 mediates binding to DDX3. To this end, we expressed different flag-tagged TRAF3 truncation mutants in HEK293T cells and immunoprecipitated them with an anti-flag antibody. In these experiments, endogenous DDX3 was pulled down with full-length TRAF3 (1-570) and the truncations 114-570 and 259-570 (Figure 1D). DDX3 did not appear to interact with TRAF3 1-381 or 389-570 (Figure 1D). Because the interaction bands observed in this IP were relatively weak, we also carried out pulldown assays with recombinant His-tagged DDX3 coupled to Ni-Agarose beads and lysates from HEK293T cells expressing the different flag-tagged truncation mutants. These pulldown experiments confirmed results from the immunoprecipitation, with TRAF3 1-570 (full-length), 114-570 and 259-570 being pulled down by His-DDX3 and no interactions observed for TRAF3 1-381 and 389-570 (Figure 1E). This data suggests that the N-terminal RING-finger and Zinc-finger domains of TRAF3 are dispensable for DDX3 binding.

Identification of a TRAF3 binding motif in DDX3

Our pulldown data suggested that a region in DDX3 between aa 139 and 172 is required for TRAF3 binding (Figure 1B). Using a Eukaryotic Linear Motif (ELM) search [22], we identified a potential TRAF-binding motif within this region, namely ^{142}-PSERLE-^{147}. We mutated proline 142 (P142) and glutamic acid 144 (E144) to alanine in order to generate a TRAF-binding site mutant of DDX3 (Figure 2A). We then tested this P142A/E144A mutant in comparison to wild-type DDX3 in immunoprecipitation and pulldown assays with TRAF3 to confirm that mutation of this putative TRAF-binding motif in DDX3 prevents TRAF3 binding (Figure 2B-D). Of note, we observed that the P142A/E144E mutant migrated slightly faster in SDS-PAGE than wild-type DDX3 (Figure 2B-D). This unexpected change in apparent molecular weight occurred for both the P142A/E144E mutant generated in pCMV-HA DDX3 (used in Figure 2B and 2C) and the P142A/E144E mutant generated in the pHis DDX3 (1-408) vector (used in Figure 2D). Both constructs were independently generated and sequence verified, ruling out that this change in apparent molecular weight is due to additional mutations/truncations. To test the effect of the mutation on TRAF3 binding, we first carried out immunoprecipitations with flag-tagged TRAF3 and HA-tagged wild-type or mutant DDX3 co-expressed in HEK293T cells. When we immunoprecipitated TRAF3 with an anti-flag antibody, only wild-type DDX3 but not the P142A/E144E mutant DDX3 co-immunoprecipitated (Figure 2B). In the reciprocal immunoprecipitation, using a HA-antibody against DDX3, TRAF3 also co-immunoprecipitated only with wild-type but not mutant DDX3 (Figure 2C). Importantly, flag-tagged TRAF3 and HA-DDX3 were also expressed alone in the absence of the other binding partner to rule out non-specific pulldown by the flag or HA antibodies (lanes 1-3 in each experiment). Finally, we also generated the P142A/E144E mutation in His-tagged (1-408) DDX3 for use in pulldown assays with recombinant protein purified from E.coli. Only wild-type (wt) but not mutant (mt) His-DDX3 (1-408) coupled to Ni-agarose beads pulled down flag-TRAF3 from cell lysates (Figure 2D). In summary, three different binding assays demonstrated that mutation of the identified putative TRAF-binding motif in DDX3 abrogates the interaction with TRAF3. This further confirms a direct interaction between DDX3 and TRAF3, and we next set out to probe the functional consequences of this DDX3-TRAF3 interaction.

The DDX3-TRAF3 interaction is required for full activation of the *ifnb* promoter

DDX3 and TRAF3 are both intermediates in the signalling pathway leading to IRF3 activation and *ifnb* promoter activation downstream of anti-viral PRRs. In addition, we previously showed that DDX3 interacts directly with IKKε to promote IRF3 phosphorylation. Knockdown of DDX3 reduced IKKε– and Sendai virus-mediated IRF3 phosphorylation and *ifnb* promoter activation [6, 8]. An IKKε-TRAF3 interaction has also been shown to be required for IRF3 activation and *ifnb* promoter induction [16]. Thus, we first determined relative activation levels of the *ifnb* promoter when TRAF3, IKKε and DDX3 were expressed separately or in combination (Figure 3A). Consistent with published data, TRAF3 and DDX3 were unable to induce promoter activation by themselves (columns 2 and 3). Co-expression of DDX3 and TRAF3 was also not sufficient to induce *ifnb* promoter activation (column 6). There was a slight enhancement when IKKε and TRAF3 were co-expressed together (column 5) in accordance with previously published studies [11, 23]. DDX3 and IKKε co-expression led to a strong enhancement of *ifnb* promoter activation (about 6-fold increase compared to IKKε alone, column 8), as shown in our previous publications [6, 8]. Addition of TRAF3 enhanced this activation further, meaning that co-expression of TRAF3, IKKε and DDX3 led to strongest activation of the *ifnb* promoter (column 7).

We next compared effects of wild-type DDX3 and the P142A/E144A TRAF3-binding site mutant of DDX3 on *ifnb* promoter activation (Figure 3B and 3C). As in Figure 3A, expression of wild-type (wt) DDX3 further enhanced *ifnb* promoter activation induced by IKKε and TRAF3 co-expression (Figure 3B, dark grey bar). However, co-expression of the P142A/E144E mutant DDX3 (mt) (light grey bar) did not enhance *ifnb* promoter activation compared to activation by IKKε/TRAF3 (black bar) (Figure 3B). Similar results were obtained when *ifnb* promoter activation was induced by SeV infection, triggering the signalling pathway at the level of RIG-I and in a more physiological manner (Figure 3C). Overexpression of wild-

type DDX3 (wt) clearly enhanced SeV-induced *ifnb* promoter activation, while P142A/E144E DDX3 (mt) only showed a slight effect. Taken together, these results suggest that DDX3, IKKε and TRAF3 cooperate to achieve full activation of the *ifnb* promoter. They also demonstrate that the DDX3-TRAF3 interaction is required for DDX3 to exert its positive effect on *ifnb* promoter activation downstream of RIG-I.

DDX3 facilitates TRAF3 ubiquitination.

We next wondered whether DDX3 regulates TRAF3 activation, one of the main indicators of which is K63-linked ubiquitination. TRAF3 K63-ubiquitination is required for induction of type I interferon, with ubiquitination most likely mediated by TRAF3's own E3 ligase activity (auto-ubiquitination) following its oligomerisation. Thus, we tested whether DDX3 affects TRAF3 ubiquitination. For initial experiments, we used an overexpression construct for Ha-tagged ubiquitin mutated at all lysine residues apart from Lysine 63 (K63-only ubiquitin, K63o), which can therefore only be incorporated into K63-linked ubiquitin chains. We co-expressed flag-tagged TRAF3 and low levels of this K63o ubiquitin construct, and stimulated RIG-I signalling by infection with Sendai Virus (SeV). Activation of the RIG-I pathway by SeV led to the appearance of a typical ubiquitination smear in the flag-TRAF3 blot (Figure 4A, lane 2), and co-expression of DDX3 enhanced this ubiquitination smear in both uninfected and SeV-infected cells (Figure 4A, lanes 3 and 4). We next wanted to determine which region(s) of DDX3 are required for its effect on TRAF3 ubiquitination, and tested our N-terminal and C-terminal DDX3 truncation mutants. Overexpression of flag-TRAF3 caused a certain level of TRAF3 ubiquitination in the absence of stimulation, due to TRAF3 oligomerisation and autoubiquitination, and full-length DDX3 (1-662) enhanced this in the absence of SeV infection (Figure 4A and 4B). To focus on direct effects of DDX3 on TRAF3, we tested the DDX3 truncations in this setting. DDX3 (aa 139-662), which lacks the N-terminal IKKϵ binding site, was still able to facilitate TRAF3 ubiquitination, while a C-terminal truncation mutant, DDX3 (aa 1-408), was unable to do so, despite retaining TRAF3 and IKKϵ binding sites. Consistently, the DDX3 (aa 172-408) truncation also failed to enhance TRAF3 ubiquitination (Figure 4B). This data suggests that, along with its TRAF-interaction motif, DDX3 also requires its C-terminal region between aa 409 and 662 to facilitate TRAF3 ubiquitination. Next, we wanted to confirm the involvement of endogenous DDX3 in TRAF3 ubiquitination, by using a cell line stably transduced with an inducible DDX3 shRNA plasmid to knock down DDX3 expression (Figure 4C). In cells transduced with a non-silencing control (NSC) shRNA, TRAF3 ubiquitination was again triggered by its overexpression (lane 1), and SeV infection slightly enhanced this (lane 2). The DDX3 knockdown we achieved was suboptimal, however TRAF3 autoubiquitination was still strongly reduced in DDX3 shRNA cells, both in the absence and presence of SeV infection (Figure 4C, lanes 3 and 4). We then wanted to confirm the importance of the TRAF3-interaction motif in DDX3 for regulating TRAF3 ubiquitination. Thus, we transfected DDX3 knockdown cells with an shRNA-resistant DDX3 expression construct for either wild-type DDX3 or the P142A/E144A TRAF3-binding site mutant of DDX3 (Figure 4D). TRAF3 overexpression resulted in strong TRAF3 autoubiquitination in NSC cells (Figure 4D, lane 1) but not DDX3 knockdown cells (Figure 4D, lane 4) as in Figure 4C. Reconstitution of knockdown cells with wild-type DDX3 restored TRAF3 ubiquitination (Figure 4D, lane 2), while reconstitution with the P142A/E144A TRAF3-binding site mutant of DDX3 did not (Figure 4D, lane 3). This suggests that a direct interaction between DDX3 and TRAF3 mediated by the TRAF-binding motif in the N-terminus of DDX3 is required for TRAF3 ubiquitination.

Finally, we wanted to verify that DDX3 is indeed involved in mediating K63-linked ubiquitination of endogenous TRAF3 following stimulation of the RIG-I pathway, as our previous experiments were carried out with overexpressed TRAF3 and K63o ubiquitin. For Figure 4E, we therefore infected non-silencing control (NSC) cells and cells containing the DDX3 shRNA with SeV for different periods of time. We then immunoprecipitated endogenous TRAF3 from denatured cell lysates (ensuring that no cellular binding partners co-immunoprecipitate), and probed these samples in a western blot with an antibody specific for K63-ubiquitin chains, thus detecting endogenous K63-linked ubiquitin chains on endogenous TRAF3. Interestingly, we observed two waves of K63-linked TRAF3 ubiquitination in SeV-infected control (NSC) cells (Figure 4E): TRAF3 was K63-ubiquitinated 15-30min following SeV infection; ubiquitination had disappeared by the 1h time point, and re-appeared at the 2h and 4h time points following infection. In cells

with DDX3 knockdown, both early and late ubiquitination of TRAF3 was impaired (Figure 4E), confirming that DDX3 is indeed required for K63-linked ubiquitination of endogenous TRAF3 in the RIG-I pathway.

DDX3 facilitates TRAF3 recruitment to MAVS

As we have now demonstrated that DDX3 directly interacts with TRAF3 as well as IKKϵ and IRF3 [6] to facilitate *ifnb* promoter induction, we wondered in which order endogenous DDX3-, TRAF3- and IKKϵ-containing signalling complexes form following stimulation of the RIG-I pathway. Investigation of endogenous signalling complexes downstream of RIG-I is not trivial due to the low expression levels of some signalling intermediates (such as IKKε) and the quality of available antibodies. Very few studies are therefore available that describe the spatiotemporal formation of endogenous signalling complexes. We switched to A549 cells for these experiments, because they have a higher expression level of IKKε than HEK293s and we previously successfully immunoprecipited endogenous DDX3-IKKε-IRF3 complexes from these cells [6]. We infected A549 cells with SeV for time periods between 15min and 2h, followed by immunoprecipitation of endogenous DDX3 or endogenous TRAF3. We had difficulties to clearly detect IKKε and TRAF3 in cell lysates, however bands at the expected molecular weight were detected in immunoprecipitated samples, where their levels are expected to be enriched. The MAVS antibody detected two specific bands, around 75 and 52 kDa, as previously described (Figure5 A-D) [24, 25]. The larger form presumably represents full-length MAVS and the other might represent the described MiniMAVS protein that lacks the N-terminal CARD domain [26].

In these experiments, immunoprecipitation of endogenous DDX3 revealed that it is recruited to MAVS within 15min of SeV infection, while the interaction had disappeared by the 2h time point after infection (Figure 5A, top panel). IKKϵ co-immunoprecipitated with DDX3 30min-2h after SeV infection, thus this interaction appeared to be slightly delayed compared to the DDX3-MAVS interaction (Figure 5A, second panel). We were unable to detect the endogenous DDX3-TRAF3 interaction when immunoprecipitating with the DDX3 antibody. However, this interaction was clearly visible when we immunoprecipitated TRAF3, namely at 1h and 2h following SeV infection (Figure 5A, third panel). MAVS also co-immunoprecipitated with TRAF3 at the same time points (Figure 5A, top panel), and IKKϵ co-immunoprecipitated at the 2h time point after SeV infection (Figure 5A, second panel). We next decided to extend the infection period to 4h in order to investigate IRF3 recruitment. In our previous study, we observed IRF3 recruitment to DDX3 and IRF phosphorylation at this time point [6]. In order to fit all samples onto one gel, important for correctly identifying and directly comparing bands, we omitted the 15min time point for this new set of experiments. Immunoprecipitation of DDX3 again revealed that the DDX3-MAVS interaction occurs early and transiently, as it was lost by 2h after infection, while the DDX3-IKKϵ interaction persisted and increased at the 2h and 4h time points (Figure 5B, top and second panel). In TRAF3 immunoprecipitations, we observed a transient interaction between TRAF3 and MAVS 1h and 2h after infection, which had disappeared by the 4h time point, thus delayed compared to the DDX3-MAVS interaction (Figure 5B, top panel). The TRAF3-IKKϵ interaction was first detectable 2h after infection, but in contrast to the MAVS interaction persisted at the 4h time point (Figure 5B, second panel). The TRAF3-DDX3 interaction was present between 1h and 4h following SeV infection (Figure 5B, third panel). Importantly, the DDX3-IRF3 and TRAF3-IRF3 interactions were first detectable 4h after SeV infection (consistent with our previous study), at a time when both proteins have been released from MAVS (Figure 5B, bottom panel). In summary, these endogenous immunoprecipitations revealed an interesting temporal sequence of the recruitment and release of DDX3, IKKϵ and TRAF3 to the MAVS adaptor molecule following activation of the RIG-I pathway (summarised in Figure 7). It appears that recruitment of DDX3 to MAVS is an early event (the only interaction we detected already 15min after infection, Figure 5A). It was therefore conceivable that DDX3 might facilitate recruitment of other signalling molecules, such as IKKϵ and TRAF3, into the MAVS complex. In order to test this hypothesis, we immunoprecipitated TRAF3 from cells subjected to shRNA knockdown of DDX3. In control cells (NSC), DDX3, MAVS and IKKϵ co-immunoprecipitated with TRAF3 1h after SeV infection as in our previous experiments. However, in DDX3 knockdown cells (shDDX3), neither MAVS nor IKKϵ co-immunoprecipitated with TRAF3 (Figure 5C).

This suggested that DDX3 is required to facilitate TRAF3 recruitment to MAVS, where it might subsequently interact with IKKϵ. On the other hand however, we then also tested whether DDX3 interactions are preserved in TRAF3 knockdown cells. To this end, we knocked down TRAF3 expression using an siRNA SMARTpool, followed by immunoprecipitation of DDX3. To our surprise, knockdown of TRAF3 also prevented the DDX3-MAVS interaction, while the DDX3-IKKε interaction was at least partially preserved (Figure 5D). This data suggest a mutual regulation between DDX3 and TRAF3, as neither appears to stably interact with MAVS in the absence of the other.

The E3 ligase activity of TRAF3 is required for MAVS binding and IRF3 recruitment

As DDX3 enhanced TRAF3 ubiquitination, we also wished to address the importance of ubiquitination for the TRAF3 interactions we observed in Figure 5. To this end, we used a TRAF3 mutant deficient in E3 ligase activity (C68A/H70A) [15], which is therefore unable to mediate ubiquitination of its substrates, including its own auto-ubiquitination. Ectopic expression of the wild-type TRAF3 construct led to spontaneous ubiquitination, which was enhanced slightly following SeV infection, while the C68A/H70A mutant did not display ubiquitination smears (Figure 6, bottom left panel, in whole cell lysates). We then immunoprecipitated wild-type TRAF3 (wt) or C68A/H70A TRAF3 using a flag-antibody and compared the co-immunoprecipitated proteins. As seen before, MAVS, DDX3, IKKϵ and IRF3 co-immunoprecipitated with wild-type TRAF3 at various time points following SeV infection (Figure 6). Interestingly, the TRAF3 C68A/H70A mutant was strongly impaired in its ability to interact with MAVS (Figure 6, top right panel). Despite this, the TRAF3-IKKϵ and TRAF3-DDX3 interactions seemed to be largely unaffected by the C68A/H70A mutation (Figure 6, panels 2 and 3). Another striking difference between wild-type TRAF3 and the C68A/H70A mutant was that IRF3 did not co-immunoprecipiate with the C68A/H70A mutant at the 4h time point after SeV infection (Figure 6, fourth panel on the right). This suggests that the E3 ligase activity/auto-ubiquitination of TRAF3 is required for its interaction with MAVS and also for recruitment of IRF3 into a separate soluble TRAF3 complex.

Discussion

In previous studies, we demonstrated that DDX3 mediates *ifnb* promoter activation following RIG-I engagement by SeV infection, and that it binds directly to IKKϵ and IRF3 in order to facilitate IRF3 activation. This study adds another layer of complexity and suggests that DDX3 might coordinate assembly of several different multiprotein signalling complexes in the RIG-I pathway. We demonstrate that DDX3 directly binds to TRAF3, which was required for DDX3 to enhance *ifnb* promoter activation. Mechanistically, our data indicates that DDX3 facilitates TRAF3 (auto)-ubiquitination and formation of a stable MAVS-TRAF3 signalling complex. Importantly, knockdown of DDX3 prevented endogenous K63-linked ubiquitination of TRAF3 and formation of a signalling complex between endogenous TRAF3 and MAVS.

The interaction between DDX3 and TRAF3

We identified a novel TRAF3-binding motif in the intrinsically disordered N-terminal region of DDX3. This motif is conserved between DDX3X (the paralogue we investigated here) and DDX3Y, as well as DDX3 orthologues in other species. Mutation of this short linear motif in DDX3 abrogated TRAF3 binding and the ability of DDX3 to facilitate TRAF3 ubiquitination and enhance activation of the *ifnb* promoter. This clearly demonstrates that direct binding between DDX3 and TRAF3 is required for *ifnb* induction downstream of RIG-I. The C-terminus of DDX3 (aa 409-662) was also required for its effect on TRAF3 ubiquitination. We can only speculate why this might be the case. There is some evidence that DDX3 might oligomerise through its C-terminal domain [27], and this could help to facilitate TRAF3 oligomerisation or the assembly of a multiprotein signalling complex. The C-terminus of DDX3 also contains a second binding site for IKKε [6] and a MAVS binding site [20]. Thus, it is also possible that DDX3 mediates a functional interaction between TRAF3 and IKKε and/or MAVS that is required for TRAF3 autoubiquitination. In any case, DDX3 likely enhances TRAF3 ubiquitination through the assembly or stabilisation of a protein

complex, as DDX3 itself does not have E3 ligase activity: it either facilitates TRAF3 autoubiquitination or recruitment of another E3 ligase that ubiquitinates TRAF3. Mapping of the DDX3 binding site on TRAF3 showed that DDX3 binds to the C-terminus of TRAF3, which contains the TRAF domain. Specifically, DDX3 binding mapped to the TRAF-N domain, which mediates oligomerisation [14]. TRAF3 oligomerisation is thought to trigger autoubiquitination [14], so this also supports our idea that DDX3 might facilitate TRAF3 autoubiquitination by promoting its oligomerisation.

Sequential recruitment of signalling molecules to MAVS

In co-immunoprecipitation experiments from SeV-infected cells, we analysed the spatiotemporal formation of different TRAF3-, IKKε-, MAVS- and DDX3-containing signalling complexes following activation of the RIG-I pathway. Importantly, these are all fully endogenous protein interactions formed in response to physiological stimulation of RIG-I by SeV infection. The DDX3-MAVS interaction was the earliest interaction we were able to detect (15min after SeV infection), which suggested that DDX3 might be involved in recruiting downstream signalling molecules to MAVS. Indeed, in DDX3 knockdown cells, TRAF3 failed to bind MAVS and IKKε (Figure 5C). However, to our complete surprise, in the reciprocal experiment, siRNA knockdown of TRAF3 also completely prevented DDX3 binding to MAVS (Figure 5D), suggesting their relationship in this signalling pathway is not of a clear linear nature. Indeed, it has previously been shown that TRAF3 can directly bind to MAVS through TRAF interaction motifs (TIMs) in the N-terminal (aa 143-147) and C-terminal (aa 455-460) regions of MAVS [13, 28]. Saha *et al.* detected a constitutive interaction between TRAF3 and MAVS, whereas Paz et al. showed a SeV-inducible interaction between MAVS and a higher molecular weight form of TRAF3, presumably ubiquitinated TRAF3 [13, 28]. Upon closer examination of our co-IP data, we also observed a weak constitutive interaction between the lower molecular weight form of MAVS and TRAF3 in some experiments (e.g. in Figure 5B). Interestingly, the E3 ligase-deficient C68/70A mutant of TRAF3 also displayed this weak constitutive interaction with MAVS, suggesting that it does not require TRAF3 ubiquitination (Figure 6). We are thus proposing the following model (Figure 7): 1. An initial weak ubiquitin-independent interaction between MAVS and TRAF3 is required for recruiting DDX3 to MAVS, explaining why the DDX3-MAVS interaction was abolished in cells with TRAF3 knockdown. 2. DDX3 and IKKε are recruited following SeV infection and interact functionally with TRAF3 to support its ubiquitination. This early TRAF3 ubiquitination (as observed in Figure 4E) stabilises and/or re-organises the signalling complex with MAVS, making it much more readily detectable in our co-IPs. In DDX3 knockdown cells, TRAF3 ubiquitination is impaired and the (strong) MAVS-TRAF3 interaction cannot be detected (Figure 2C-E, Figure 5C). 3. DDX3 and TRAF3 are released from MAVS, but continue to interact with each other and with IKKε (Figure 5A and B). We hypothesise that removal of K63-ubiquitination from TRAF3 might be required for release from MAVS (based on our data in Figure 4E, where TRAF3 ubiquitination disappeared around 1h after infection). We detected DDX3-IRF3 and TRAF3-IRF3 interactions at the 4h timepoint (Figure 5B). This corresponds to the time frame when IRF3 phosphorylation takes place [6], suggesting that activation of IRF3 most likely occurs in this soluble signalling complex containing IKKε, TRAF3, and DDX3. We cannot conclude with certainty that these proteins are all present in the same multiprotein complex rather than in several separate complexes, but due to the presence of non-overlapping binding sites for TRAF3, IKKε and IRF3 in DDX3 and the potential for oligomerisation it is a conceivable possibility. This soluble complex also coincided with the second wave of TRAF3 ubiquitination we observed 2-4h after SeV infection (Figure 4E) and we therefore hypothesise that this ubiquitination is required for IRF3 recruitment. This is also supported by our finding that the E3 ligase-deficient C68/70A mutant of TRAF3 did not interact with IRF3 4h after SeV infection (Figure 6).

The role of TRAF3 (ubiquitination) in interferon induction

While it is widely accepted that TRAF3 is an essential component in signalling pathways leading to IRF3 activation and IFN-β induction [11, 29], its exact role in these pathways is still rather unclear. Most studies suggest that TRAF3 mediates recruitment of IKKϵ/TBK1 to upstream adaptor molecules, such as MAVS,

and thus activation of these kinases [11, 23, 30, 31]. Auto-ubiquitination of TRAF3 is required for IRF3 activation and *ifnb* promoter induction [15], and several studies suggest that this ubiquitination mediates TRAF3 binding to IKKϵ/TBK1 [16, 23, 30, 32]. It has also been suggested that IKKϵ/TBK1 are ubiquitinated by TRAF3, with that ubiquitination being required for IKKε/TBK1-mediated IRF3 activation and IFN induction [23, 33, 34]. However, it has more recently been suggested that TRAF3 is not required for IKKϵ/TBK1 activation, but that it rather mediates IRF3 activation downstream of these kinases [5]. So, does TRAF3 act upstream or downstream of IKKε/TBK1? And what role does TRAF3 ubiquitination play? Our study did not set out to answer these questions, but it provides several novel insights and a potential explanation for the discrepancies in published findings. Our data suggest that the signalling pathway downstream of MAVS is by no means linear, as illustrated by our findings in DDX3 and TRAF3 knockdown cells. TRAF3 is recruited into different protein complexes as signalling events downstream of MAVS progress, thus timing of experiments will greatly influence results. We propose that early (auto)-ubiquitination of TRAF3 stabilises a signalling complex with MAVS. It is conceivable that this signalling complex contributes to the full and/or sustained activation of IKKε/TBK1. For example, TRAF3 knockdown prevented DDX3 recruitment to MAVS and the DDX3-IKKε interaction also appeared to be more transient in TRAF3 knockdown cells (Figure 5D). Seeing as we have previously shown that DDX3 enhances IKKε activation in SeV-infected cells [6], TRAF3 could hereby indirectly affect IKKε/TBK1 activation in the RIG-I pathway. At the 4h time point after infection, TRAF3 had been released from MAVS, but continued to interact with IKKε and DDX3 and started to interact with IRF3 (Figure 5B). Importantly, the E3-ligase deficient mutant of TRAF3 did not interact with IRF3 under these conditions (Figure 6), clearly indicating a role for TRAF3 (ubiquitination) in IRF3 recruitment (and therefore presumably activation). In alignment with this interaction data, we detected two waves of K63-linked TRAF3 ubiquitination after SeV-infection, and we suggest that these correspond to its involvement in these distinct signalling events. The early wave, observed 15-30min after infection, is likely to stabilise the interaction with MAVS, which was also defective with the E3-ligase deficient mutant of TRAF3. Late K63-linked TRAF3 ubiquitination occurred 2-4h after infection and is likely to support IRF3 recruitment and activation, as discussed above.

In summary, our data suggest that TRAF3 and its ubiquitination have a dual role in RIG-I signalling, explaining why researchers have placed it at different levels in the signalling pathway in the past. Clearly, we still do not fully understand the complexities of the RIG-I signalling pathway and many open questions remain regarding the role and regulation of TRAF3 in this pathway. TRAF3 is targeted by several cellular and viral deubiquitinases (DUBs), and most of them, including DUBA and HSV-1 UL36, did not block IFN induction downstream of IKKε/TBK1 [16, 32], which might suggest they specifically act on early TRAF3 ubiquitination. In future studies, it would be interesting to determine whether different DUBs target ubiquitinated TRAF3 specifically in the early versus late signalling complexes. Based on our data, we also hypothesise that TRAF3 might require deubiquitination for signalling to proceed, namely for it to be released from MAVS. It would be interesting to confirm this and to determine how this particular deubiquitination event is regulated.

It is also possible that TRAF3 ubiquitination is regulated by phosphorylation. To our knowledge, there is no experimental evidence that IKKε phosphorylates TRAF3. However, it has been shown to phosphorylate TRAF2, making it conceivable that other TRAFs could also be targets of its phosphorylation [35]. We have some evidence that inhibition of IKKε's kinase activity blocks TRAF3 ubiquitination at early time points (data not shown), suggesting that IKKε either phosphorylates TRAF3 directly or phosphorylates another protein required for TRAF3 ubiquitination. Most interestingly, CK1ε, another kinase whose kinase activity is regulated by DDX3, has recently been demonstrated to phosphorylate TRAF3 directly. This phosphorylation event promoted TRAF3 autoubiquitination and enhanced *ifnb* promoter activation [36]. Thus, it is possible that DDX3 links CK1ε and/or IKKε to TRAF3 to mediate its phosphorylation, similar to what we have described for IRF3 before, and that this promotes TRAF3 autoubiquitination [6]. However, DDX3's role in facilitating TRAF3 ubiquitination clearly goes beyond stimulating the activity of CK1ε

and/or IKKε, seeing as a direct interaction between DDX3 and TRAF3 mediated by DDX3's TRAF-binding motif is required for its effect.

DDX3 function in the RIG-I signalling pathway

While our study provides interesting novel insights into the spatiotemporal regulation of RIG-I signalling and the role of TRAF3 as discussed above, our main focus was the function of DDX3. We identified a novel direct interaction between DDX3 and TRAF3 that is mediated by an interaction motif in the flexible N-terminus of DDX3. This direct interaction between DDX3 and TRAF3 was required for TRAF3 ubiquitination, the formation of a stable MAVS-TRAF3 complex, and activation of the *ifnb* promoter. Previously, we have shown that direct DDX3-IKKε and DDX3-IRF3 interactions are also required for IRF3 activation and activation of the *ifnb* promoter [6]. Furthermore, DDX3 can also directly bind to MAVS ([20], Figure 1A and data not shown). It thus emerges that DDX3 can bridge several different interactions between important signalling molecules downstream of MAVS at different time points post infection. Our study therefore reveals the multifunctionality of DDX3 as a signalling adaptor in the RIG-I signalling pathway, reinforcing its characterisation as a key facilitator of the type I interferon induction pathway downstream of RIG-I.

Acknowledgements:

We sincerely thank Caren Bartsch and Sören Latteyer for their assistance with experiments. We also thank Profs Carl Ware and Michael Karin for TRAF3 plasmids and Prof Carl Ware for sharing unpublished data. Finally, we thank Dr Marion Butler and Prof Paul Moynagh for critical reading of the manuscript and helpful discussions.

Author Contributions

LG carried out the majority of experiments in this study, AF carried out the experiment showing endogenous TRAF3 ubiquitination, NMcC carried out pulldowns with DDX3 truncations, and YH generated DDX3 knockdown A549 cells used for this study. MS was involved in study design, planning and analysing of experiments. MS and LG co-wrote the manuscript, which was edited by AF, NMcC and YH.

References

1 Fitzgerald, K. A., McWhirter, S. M., Faia, K. L., Rowe, D. C., Latz, E., Golenbock, D. T., Coyle, A. J., Liao, S. M. and Maniatis, T. (2003) IKKepsilon and TBK1 are essential components of the IRF3 signaling pathway. Nat Immunol. **4**, 491-496

2 Sharma, S., tenOever, B. R., Grandvaux, N., Zhou, G.-P., Lin, R. and Hiscott, J. (2003) Triggering the Interferon Antiviral Response Through an IKK-Related Pathway. Science. **300**, 1148-1151

3 Johnson, C. L. and Gale Jr, M. (2006) CARD games between virus and host get a new player. Trends in Immunology. **27**, 1-4

4 Kato, H., Sato, S., Yoneyama, M., Yamamoto, M., Uematsu, S., Matsui, K., Tsujimura, T., Takeda, K., Fujita, T., Takeuchi, O. and Akira, S. (2005) Cell type-specific involvement of RIG-I in antiviral response. Immunity. **23**, 19-28

5 Clark, K., Peggie, M., Plater, L., Sorcek, R. J., Young, E. R., Madwed, J. B., Hough, J., McIver, E. G. and Cohen, P. (2011) Novel cross-talk within the IKK family controls innate immunity. Biochem J. **434**, 93-104

6 Gu, L., Fullam, A., Brennan, R. and Schröder, M. (2013) The human DEAD-box helicase 3 couples IKK-epsilon to IRF3 activation. Molecular and Cellular Biology. **33**, 2004-2015

7 Fullam, A. and Schroder, M. (2013) DExD/H-box RNA helicases as mediators of anti-viral innate immunity and essential host factors for viral replication. Biochim Biophys Acta. **1829**, 854-865

8 Schroder, M., Baran, M. and Bowie, A. G. (2008) Viral targeting of DEAD box protein 3 reveals its role in TBK1/IKK-epsilon-mediated IRF activation. Embo J. **17**, 17

9 Soulat, D., Burckstummer, T., Westermayer, S., Goncalves, A., Bauch, A., Stefanovic, A., Hantschel, O., Bennett, K. L., Decker, T. and Superti-Furga, G. (2008) The DEAD-box helicase DDX3X is a critical component of the TANK-binding kinase 1-dependent innate immune response. Embo J. **26**, 26
10 Ditton, H. J., Zimmer, J., Kamp, C., Rajpert-De Meyts, E. and Vogt, P. H. (2004) The AZFa gene DBY (DDX3Y) is widely transcribed but the protein is limited to the male germ cells by translation control. Hum. Mol. Genet. **13**, 2333-2341
11 Oganesyan, G., Saha, S. K., Guo, B., He, J. Q., Shahangian, A., Zarnegar, B., Perry, A. and Cheng, G. (2006) Critical role of TRAF3 in the Toll-like receptor-dependent and -independent antiviral response. Nature. **439**, 208-211
12 Hacker, H., Redecke, V., Blagoev, B., Kratchmarova, I., Hsu, L. C., Wang, G. G., Kamps, M. P., Raz, E., Wagner, H., Hacker, G., Mann, M. and Karin, M. (2006) Specificity in Toll-like receptor signalling through distinct effector functions of TRAF3 and TRAF6. Nature. **439**, 204-207
13 Saha, S. K., Pietras, E. M., He, J. Q., Kang, J. R., Liu, S. Y., Oganesyan, G., Shahangian, A., Zarnegar, B., Shiba, T. L., Wang, Y. and Cheng, G. (2006) Regulation of antiviral responses by a direct and specific interaction between TRAF3 and Cardif. Embo J. **25**, 3257-3263
14 Xie, P. (2013) TRAF molecules in cell signaling and in human diseases. Journal of Molecular Signaling. **8**, 7
15 Tseng, P. H., Matsuzawa, A., Zhang, W., Mino, T., Vignali, D. A. and Karin, M. (2010) Different modes of ubiquitination of the adaptor TRAF3 selectively activate the expression of type I interferons and proinflammatory cytokines. Nat Immunol. **11**, 70-75
16 Kayagaki, N., Phung, Q., Chan, S., Chaudhari, R., Quan, C., O'Rourke, K. M., Eby, M., Pietras, E., Cheng, G., Bazan, J. F., Zhang, Z., Arnott, D. and Dixit, V. M. (2007) DUBA: a deubiquitinase that regulates type I interferon production. Science. **318**, 1628-1632
17 Force, W. R., Cheung, T. C. and Ware, C. F. (1997) Dominant negative mutants of TRAF3 reveal an important role for the coiled coil domains in cell death signaling by the lymphotoxin-beta receptor. J Biol Chem. **272**, 30835-30840
18 Ryzhakov, G. and Randow, F. (2007) SINTBAD, a novel component of innate antiviral immunity, shares a TBK1-binding domain with NAP1 and TANK. Embo J. **26**, 3180-3190
19 DeFilippis, V. R., Alvarado, D., Sali, T., Rothenburg, S. and Fruh, K. (2010) Human Cytomegalovirus Induces the Interferon Response via the DNA Sensor ZBP1. J. Virol. **84**, 585-598
20 Oshiumi, H., Sakai, K., Matsumoto, M. and Seya, T. (2010) DEAD/H BOX 3 (DDX3) helicase binds the RIG-I adaptor IPS-1 to up-regulate IFN-beta-inducing potential. European Journal of Immunology. **40**, 940-948
21 Wang, H. and Ryu, W.-S. (2010) Hepatitis B Virus Polymerase Blocks Pattern Recognition Receptor Signaling via Interaction with DDX3: Implications for Immune Evasion. Plos Pathog. **6**, e1000986
22 Dinkel, H., Michael, S., Weatheritt, R. J., Davey, N. E., Van Roey, K., Altenberg, B., Toedt, G., Uyar, B., Seiler, M., Budd, A., Jodicke, L., Dammert, M. A., Schroeter, C., Hammer, M., Schmidt, T., Jehl, P., McGuigan, C., Dymecka, M., Chica, C., Luck, K., Via, A., Chatr-Aryamontri, A., Haslam, N., Grebnev, G., Edwards, R. J., Steinmetz, M. O., Meiselbach, H., Diella, F. and Gibson, T. J. (2012) ELM--the database of eukaryotic linear motifs. Nucleic Acids Res. **40**, D242-251
23 Parvatiyar, K., Barber, G. N. and Harhaj, E. W. (2010) TAX1BP1 and A20 Inhibit Antiviral Signaling by Targeting TBK1-IKKi Kinases. Journal of Biological Chemistry. **285**, 14999-15009
24 Hou, F., Sun, L., Zheng, H., Skaug, B., Jiang, Q. X. and Chen, Z. J. (2011) MAVS forms functional prion-like aggregates to activate and propagate antiviral innate immune response. Cell. **146**, 448-461
25 Seth, R. B., Sun, L., Ea, C.-K. and Chen, Z. J. (2005) Identification and Characterization of MAVS, a Mitochondrial Antiviral Signaling Protein that Activates NF-κB and IRF3. Cell. **122**, 669-682
26 Brubaker, Sky W., Gauthier, Anna E., Mills, Eric W., Ingolia, Nicholas T. and Kagan, Jonathan C. (2014) A Bicistronic MAVS Transcript Highlights a Class of Truncated Variants in Antiviral Immunity. Cell. **156**, 800-811

27 Putnam, Andrea A., Gao, Z., Liu, F., Jia, H., Yang, Q. and Jankowsky, E. (2015) Division of Labor in an Oligomer of the DEAD-Box RNA Helicase Ded1p. Molecular Cell. **59**, 541-552
28 Paz, S., Vilasco, M., Werden, S. J., Arguello, M., Joseph-Pillai, D., Zhao, T., Nguyen, T. L., Sun, Q., Meurs, E. F., Lin, R. and Hiscott, J. (2011) A functional C-terminal TRAF3-binding site in MAVS participates in positive and negative regulation of the IFN antiviral response. Cell Res. **21**, 895-910
29 Hacker, H., Tseng, P. H. and Karin, M. (2011) Expanding TRAF function: TRAF3 as a tri-faced immune regulator. Nat Rev Immunol. **11**, 457-468
30 Karim, R., Tummers, B., Meyers, C., Biryukov, J. L., Alam, S., Backendorf, C., Jha, V., Offringa, R., van Ommen, G. J., Melief, C. J., Guardavaccaro, D., Boer, J. M. and van der Burg, S. H. (2013) Human papillomavirus (HPV) upregulates the cellular deubiquitinase UCHL1 to suppress the keratinocyte's innate immune response. Plos Pathog. **9**, e1003384
31 Siu, K.-L., Kok, K.-H., Ng, M.-H. J., Poon, V. K. M., Yuen, K.-Y., Zheng, B.-J. and Jin, D.-Y. (2009) Severe Acute Respiratory Syndrome Coronavirus M Protein Inhibits Type I Interferon Production by Impeding the Formation of TRAF3·TANK·TBK1/IKKϵ Complex. Journal of Biological Chemistry. **284**, 16202-16209
32 Wang, S., Wang, K., Li, J. and Zheng, C. (2013) HSV-1 ubiquitin-specific protease UL36 inhibits IFN-β production by deubiquitinating TRAF3. Journal of Virology
33 Tu, D., Zhu, Z., Zhou, Alicia Y., Yun, C.-h., Lee, K.-E., Toms, Angela V., Li, Y., Dunn, Gavin P., Chan, E., Thai, T., Yang, S., Ficarro, Scott B., Marto, Jarrod A., Jeon, H., Hahn, William C., Barbie, David A. and Eck, Michael J. (2013) Structure and Ubiquitination-Dependent Activation of TANK-Binding Kinase 1. Cell Reports. **3**, 747-758
34 Zhou, Alicia Y., Shen, Rhine R., Kim, E., Lock, Ying J., Xu, M., Chen, Zhijian J. and Hahn, William C. (2013) IKKε-Mediated Tumorigenesis Requires K63-Linked Polyubiquitination by a cIAP1/cIAP2/TRAF2 E3 Ubiquitin Ligase Complex. Cell Reports. **3**, 724-733
35 Shen, R. R., Zhou, A. Y., Kim, E., Lim, E., Habelhah, H. and Hahn, W. C. (2012) IkappaB kinase epsilon phosphorylates TRAF2 to promote mammary epithelial cell transformation. Mol Cell Biol. **32**, 4756-4768
36 Zhou, Y., He, C., Yan, D., Liu, F., Liu, H., Chen, J., Cao, T., Zuo, M., Wang, P., Ge, Y., Lu, H., Tong, Q., Qin, C., Deng, Y. and Ge, B. (2016) The kinase CK1varepsilon controls the antiviral immune response by phosphorylating the signaling adaptor TRAF3. Nat Immunol. **17**, 397-405

Figure legends

Figure 1. DDX3 interacts directly with TRAF3.
(A) Flag-IKKϵ, flag-MAVS, flag-TRAF3, flag-Sintbad, flag-TANK or flag-NAP were ectopically expressed in HEK293T cells and cell lysates were prepared 24-48h after transfection. Recombinant GST-DDX3 or GST (as a control) coupled to Glutathione Sepharose beads were then used to pull down these flag-tagged proteins from the cell lysates. After pulldowns, beads were thoroughly washed, boiled in SDS sample buffer and subjected to SDS-PAGE and Western Blot Analysis. GST and GST-DDX3 signals were detected on the same autorad film; this is indicated by the black box around the bottom two panels. His-DDX3 coupled to Nickel-Agarose beads (NiAg) was used for the MAVS pulldown, with empty Ni-Ag beads used in the control pulldown. In all cases, cell lysates were run as input controls to confirm expression of the protein. **(B)** Recombinant His-tagged DDX3 truncation mutants coupled to Nickel-Agarose (Ni-Ag) beads were used to pull down flag-tagged TRAF3 from lysates of HEK293T cells that had been transfected with a TRAF3 expression construct for 24 h. Numbers indicate amino acid positions of DDX3 truncations, with 1-662 representing full-length DDX3. Beads were thoroughly washed, boiled in SDS sample buffer and subjected to SDS-PAGE and Western Blot analysis with anti-flag and anti-His antibodies. Empty Ni-Agarose beads (Ni-Ag) were used in a control pulldown, and expression of flag-TRAF3 in the cell lysate is shown in the input control. **(C)** Recombinant His-tagged DDX3 coupled to Nickel-Agarose beads or empty Ni-Agarose beads as a control (Ni-Ag) were incubated with 2 μg of recombinant GST-tagged TRAF3 in lysis buffer. Beads were thoroughly washed, boiled in SDS sample buffer and subjected to SDS-PAGE

and Western Blot Analysis with anti-TRAF3 and anti-His antibodies. **(D)** Expression constructs for different flag-tagged TRAF3 truncations were transfected into HEK293T cells, as indicated (numbers represent amino acid positions). 1-570 represents full-length TRAF3. 24 h after transfection, cells were lysed and TRAF3 truncations were immunoprecipitated using anti-flag M2 Agarose. Immunoprecipitates were thoroughly washed, boiled in SDS sample buffer and subjected to SDS-PAGE and Western Blot analysis with antibodies against endogenous DDX3 and the flag epitope tag. L.C.: antibody light chain. **(E)** Full-length flag-tagged TRAF3 (1-570) or different TRAF3 truncation mutants were ectopically expressed in HEK293T cells and cell lysates were prepared 24 h after transfection. Recombinant His-DDX3 coupled to Nickel-Agarose beads was then used to pull down flag-tagged TRAF3 truncations from cell lysates. Precipitates were thoroughly washed, boiled in SDS sample buffer and subjected to SDS-PAGE and Western Blot analysis with the indicated antibodies. Expression of the different TRAF3 constructs in cell lysates is confirmed in the right panel (Input) and equal pulldown of His-DDX3 across all samples is confirmed in the bottom left panel.

Figure 2. An N-terminal TRAF-binding motif in DDX3 mediates TRAF3 binding
(A) Through an ELM (eukaryotic linear motif) search, we identified a putative TRAF binding motif between amino acid 141 and 147 in human DDX3(X). To test the functional importance of this motif, we mutated the proline (P) at position 142 and the glutamic acid (E) at position 144 to alanines (A) (142/144A mutant). **(B)** Expression constructs for flag-TRAF3 and either Ha-DDX3 or the Ha-DDX3 P142/E144A mutant were transfected alone or in combination into HEK293T cells. 24 h after transfection, cells were lysed and TRAF3 was immunoprecipitated using anti-flag M2 Agarose. Immunoprecipitates were thoroughly washed, boiled in SDS sample buffer and subjected to SDS-PAGE and Western Blot analysis with the indicated antibodies. **(C)** As in (A), but Ha-DDX3 was immunoprecipitated with an anti-Ha antibody absorbed to Protein G sepharose. **(D)** Recombinant His-tagged DDX3 (1-408) coupled to Nickel-Agarose (Ni-Ag) beads was used to pull down flag-tagged TRAF3 from lysates of HEK293T cells that had been transfected with a TRAF3 expression construct for 24 h. His-tagged 1-408 wildtype (wt) DDX3 was compared to 1-408 DDX3 carrying the P142/E144A mutation (mt), and empty Ni-Agarose beads were used in a control pulldown (Ni-Ag). Beads were thoroughly washed, boiled in SDS sample buffer and subjected to SDS-PAGE and Western Blot analysis with the indicated antibodies. TRAF3 expression in cell lysates is shown as an input control; and input and pulldown samples were detected on the same autorad film as indicated by the black box around the top panel.

Figure 3. TRAF3 binding of DDX3 is required for *ifnb* promoter induction.
(A) HEK293T cells were transfected with an *ifnb* promoter firefly luciferase reporter gene construct, a Renilla control luciferase construct, and expression constructs for flag-IKKε, flag-TRAF3, and Ha-DDX3 alone or in combination. Luciferase activity was measured 24h after transfection. Data are normalised to Renilla luciferase levels and expressed as mean fold induction relative to control levels ± standard deviation. Shown is one representative experiment of three, performed in triplicate. **(B)** The effects of wild-type DDX3 (wt) (dark grey bar) and the P142/E144A Ha-DDX3 mutant (mt) (light grey bar) are compared on TRAF3/IKKε–induced *ifnb* promoter activity measured by luciferase reporter assays as described in (A). Activation levels induced by TRAF3 (T3) and IKKε alone are also shown for reference. **(C)** As in (B), but *ifnb* promoter activation was induced by infection with Sendai Virus (SeV) 16 h before measuring luciferase levels.

Figure 4. DDX3 facilitates K63-linked TRAF3 ubiquitination
(A) HEK293T cells were transfected with expression constructs for flag-TRAF3 and K63o Ubiquitin, with or without Ha-DDX3 as indicated. Cells were infected with SeV 30min prior to cell lysis where indicated. Cell lysates were subjected to SDS-PAGE and Western Blot Analysis with an anti-flag antibody (to detect TRAF3) and anti-Ha antibody (to detect DDX3). **(B)** As in (A), but cells were transfected with empty vector (EV) or expression constructs for either full-length Ha-DDX3 (1-662) or different Ha-tagged N- or C-terminal DDX3 truncation mutants (numbers indicate amino acid positions). Expression of these

truncations was confirmed by anti-Ha western blot on cell lysates (bottom panel). **(C)** DDX3 knockdown was induced in HEK293T cells stably transfected with pTRIPZ-shDDX3 (or a non-silencing control (NSC) pTRIPZ vector) through incubation with 0.5 ug/ml doxycyline for 48 h. 24 h after doxycycline addition, cells were transfected with expression constructs for flag-TRAF3 and Ha-K63o Ubiquitin. Cells were infected with SeV 30 min prior to cell lysis. Cell lysates were prepared and subjected to SDS-PAGE and Western Blot Analysis with anti-flag and anti-DDX3 antibodies. **(D)** As in (C), but DDX3 expression was reconstituted by co-transfection of shRNA-resistant expression constructs for either wildtype DDX3 (wt) or the 142/144A DDX3 mutant (mt). Similar expression levels of the wild-type and mutant DDX3 were confirmed by anti-Ha western blot (bottom panel). **(E)** DDX3 knockdown was induced in HEK293T shDDX3 cells (or NSC controls) as in (C) and (D). Cells were then infected with SeV for the indicated periods of time. Cell lysates were prepared and boiled with SDS for 5 min to disrupt protein complexes. Subsequently, endogenous TRAF3 was immunoprecipitated and analysed by SDS-PAGE and Western Blot Analysis with an antibody specific for K63-linked ubiquitin chains. DDX3 knockdown was confirmed by western blotting on cell lysates, with anti-tubulin staining serving as loading control (bottom panel). Samples from NSC and shDDX3 cells were analysed on the same gel/blot, as indicated by the black boxes around panels.

Figure 5. Spatiotemporal formation of different endogenous DDX3- and TRAF3-containing signalling complexes following RIG-I activation.
(A and B) A549 cells were infected with SeV for the indicated time periods. Cell lysates were then prepared and either endogenous DDX3 or endogenous TRAF3 were immunoprecipitated. Immunoprecipitates (IP) were washed thoroughly and subjected to SDS-PAGE and Western Blot (WB) analysis with MAVS, IKKε, DDX3 and TRAF3 antibodies. In **(B)** IRF3 recruitment was also analysed by western blotting. The MAVS antibody detected two bands, which presumably represent full-length MAVS and the shorter MiniMAVS protein. IKKε and TRAF3 were difficult to detect in cell lysates, but bands at the correct molecular weight were detected in immunoprecipiations where they are expected to be enriched. All samples from one experiment (lysates and both immunoprecipitates) were run on the same gel/blot to allow for correct identification and direct comparison of bands. H.C.: antibody heavy chain, ns: non-specific band **(C)** DDX3 knockdown was induced in A549 cells stably transfected with pTRIPZ-shDDX3 (or a non-silencing control (NSC) pTRIPZ vector) through incubation with 0.5 μg/ml doxycyline for 48h. Cells were then infected with SeV for the indicated time periods, followed by preparation of cell lysates and immunoprecipitation of endogenous TRAF3. Immunoprecipitates were washed thoroughly and subjected to SDS-PAGE and Western Blot Analysis with MAVS, IKKε, DDX3 and TRAF3 antibodies. Lysates and IP samples were run on the same gel/blot and visualised on the same autorad, indicated by the black boxes around the panels. **(D)** A549 cells were transfected with TRAF3 siRNA (siTRAF3) or a non-silencing control oligo (NSC). Cells were infected with SeV for the indicated periods of time, and harvested 48 h after siRNA transfection. DDX3 was immunoprecipitated from cell lysates and immunoprecipitates were analysed by SDS-PAGE and Western Blot Analysis with MAVS, IKKε, DDX3 and TRAF3 antibodies. Lysates and IP samples were run on the same gel/blot and visualised on the same autorad, indicated by the black boxes around the panels.

Figure 6. TRAF3 E3 ligase activity is required for MAVS and IRF3 interaction. A549 cells were transfected with either flag-tagged wild-type (wt) TRAF3 or the E3-ligase deficient C68A/H70A mutant. 24 h after transfection, cells were infected with SeV for the indicated time periods, followed by preparation of cell lysates and immunoprecipitation of flag-TRAF3 with anti-flag M2 agarose. Immunoprecipitates were washed thoroughly and subjected to SDS-PAGE and Western Blot Analysis with MAVS, IKKε, DDX3, TRAF3 and IRF3 antibodies. Samples from wild-type (wt) and C68A/H70A mutant TRAF3-transfected cells were run side-by-side on the same gel/blot, for both cell lysates (Input, left panels) and immunoprecipitates (IP, right panel) to ensure that we can directly compare bands for wild-type and mutant TRAF3.

Figure 7: Schematic summary of signalling events observed following stimulation of the Rig-I pathway. This schematic summarises the sequential interactions we observed when we immunoprecipitated endogenous DDX3 (black bars) or endogenous TRAF3 (grey bars) at different time points following SeV infection (Figures 5A and B). It also gives an indication of the temporal occurrence of TRAF3 ubiquitination as observed in Fig 4E (dark grey bars), and IKKϵ and IRF3 phosphorylation as previously observed (Gu *et al*, MCB 2013), in relation to these interactions. The drawing illustrates the composition of the different signalling complexes we propose based on our co-IP data. At the 4 h time point, DDX3, IKKε and TRAF3 no longer interact with MAVS, but are interacting instead with IRF3. This suggests the presence of a soluble signalling complex that contains DDX3, IKKε, TRAF3 and IRF3 and facilitates IRF3 activation. Formation of the MAVS-bound complex and the IRF3-containing complex seem to correlate with the early and late wave of K63-linked TRAF3 ubiquitination we observed. This is further supported by our finding that E3-ligase-deficient non-ubiquitinated TRAF3 did not interact with MAVS or IRF3 following SeV stimulation (Figure 6).

Figure 1

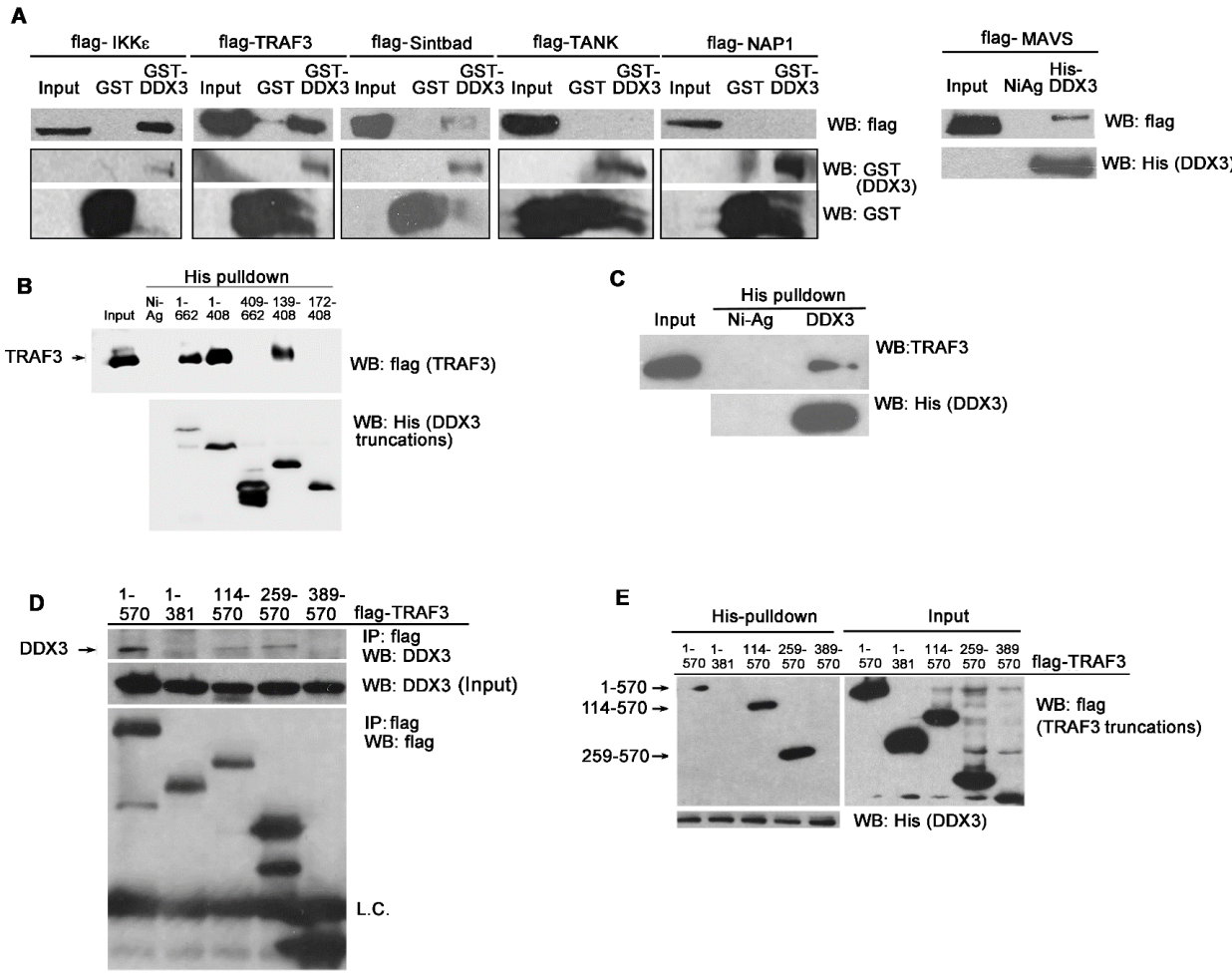
A
flag- IKKε
flag-TRAF3
flag-Sintbad
flag-TANK
flag- NAP1
flag- MAVS
Input
GST
GST-DDX3
His-DDX3
NiAg
WB: flag
WB: GST (DDX3)
WB: GST
WB: His (DDX3)
B
His pulldown
Ni-Ag
1-662
1-408
409-662
139-408
172-408
TRAF3
WB: flag (TRAF3)
WB: His (DDX3 truncations)
C
His pulldown
Ni-Ag
DDX3
WB:TRAF3
WB: His (DDX3)
D
1-570
1-381
114-570
259-570
389-570
flag-TRAF3
DDX3
IP: flag
WB: DDX3
WB: DDX3 (Input)
IP: flag
WB: flag
L.C.
E
His-pulldown
Input
1-570
114-570
259-570
389-570
flag-TRAF3
WB: flag (TRAF3 truncations)
WB: His (DDX3)

Figure 2

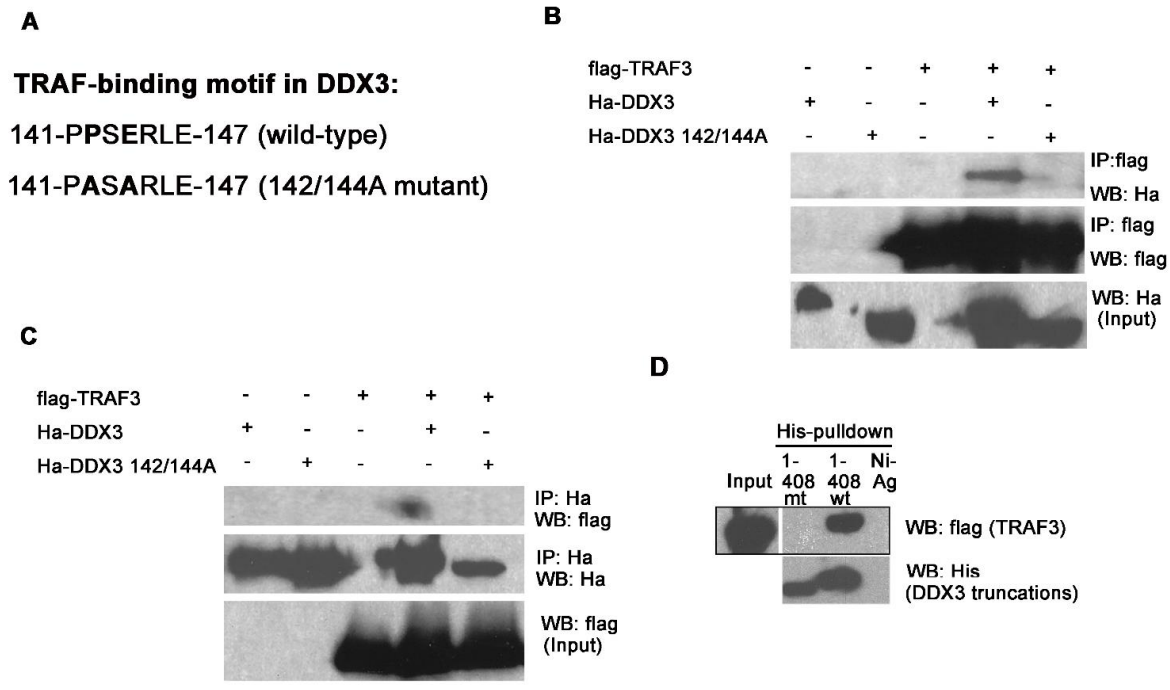
A
TRAF-binding motif in DDX3:
141-PPSERLE-147 (wild-type)
141-PASARLE-147 (142/144A mutant)
B
flag-TRAF3 - - + + +
Ha-DDX3 + - - + -
Ha-DDX3 142/144A - + - - +
IP:flag
WB: Ha
IP: flag
WB: flag
WB: Ha
(Input)
C
flag-TRAF3 - - + + +
Ha-DDX3 + - - + -
Ha-DDX3 142/144A - + - - +
IP: Ha
WB: flag
IP: Ha
WB: Ha
WB: flag
(Input)
D
His-pulldown
Input
1-408 mt
1-408 wt
Ni-Ag
WB: flag (TRAF3)
WB: His
(DDX3 truncations)

Figure 3

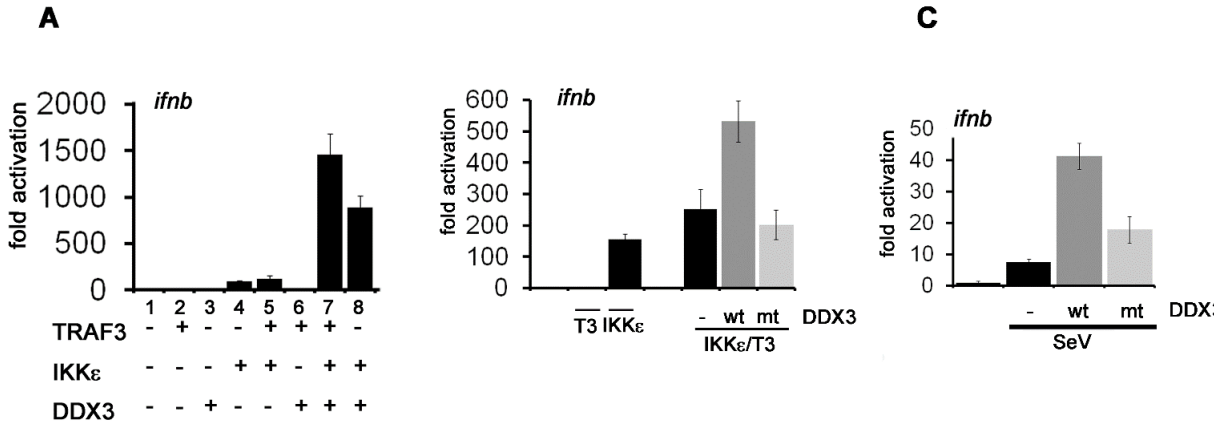

Figure 4

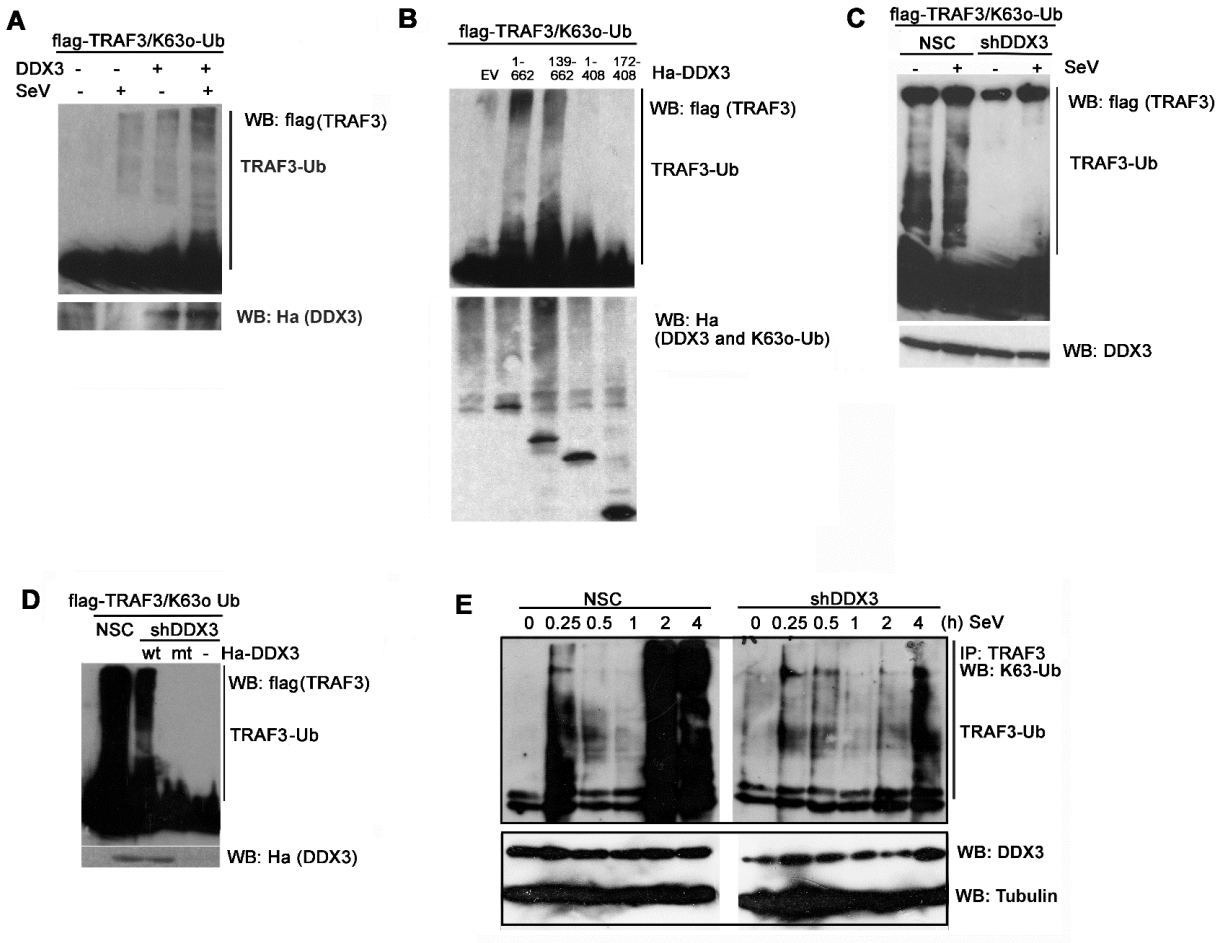

Figure 5

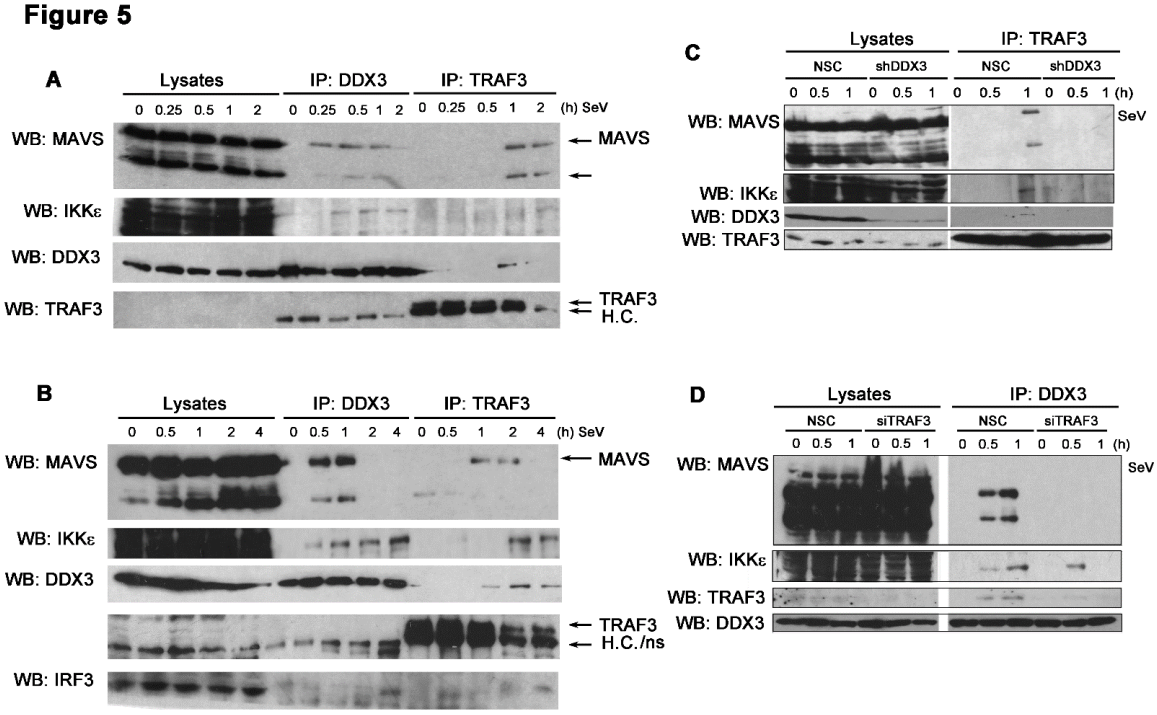

Figure 6

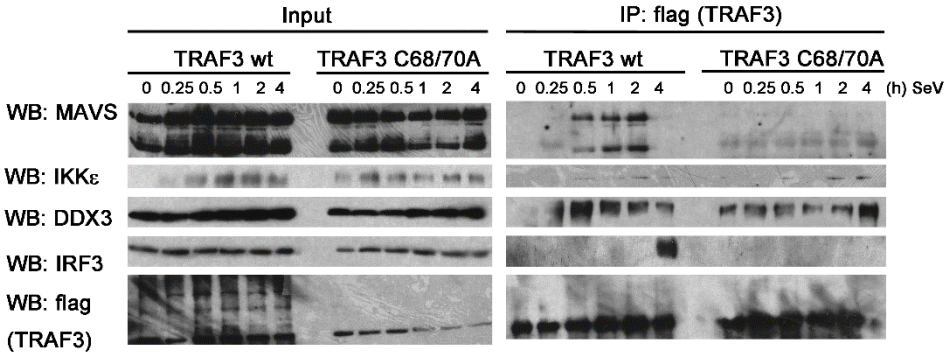

Figure 7

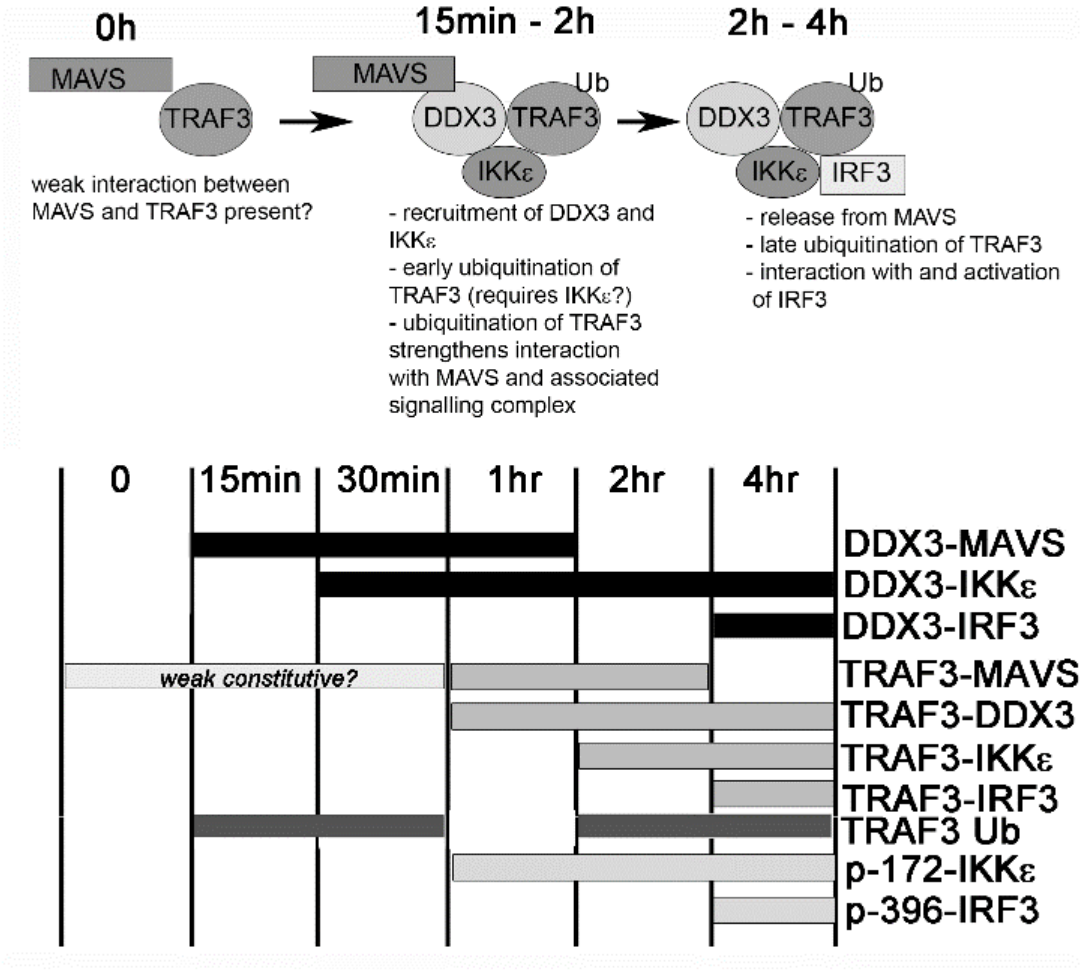
0h
15min - 2h
2h - 4h
MAVS
TRAF3
MAVS
Ub
DDX3
TRAF3
IKKε
Ub
DDX3
TRAF3
IKKε
IRF3
weak interaction between MAVS and TRAF3 present?
- recruitment of DDX3 and IKKε
- early ubiquitination of TRAF3 (requires IKKε?)
- ubiquitination of TRAF3 strengthens interaction with MAVS and associated signalling complex
- release from MAVS
- late ubiquitination of TRAF3
- interaction with and activation of IRF3
0
15min
30min
1hr
2hr
4hr
DDX3-MAVS
DDX3-IKKε
DDX3-IRF3
TRAF3-MAVS
TRAF3-DDX3
TRAF3-IKKε
TRAF3-IRF3
TRAF3 Ub
p-172-IKKε
p-396-IRF3
weak constitutive?